Multiwalled Carbon Nanotubes by Chemical Vapor Deposition Using Multilayered Metal Catalysts

Lance Delzeit,* Cattien V. Nguyen,† Bin Chen,† Ramsey Stevens,† Alan Cassell,† Jie Han,† and M. Meyyappan

NASA Ames Research Center, Moffett Field, California 94035

Received: February 8, 2002; In Final Form: March 28, 2002

Multiwalled carbon nanotubes (MWCNTs) have been grown on various substrates by thermal chemical vapor deposition using multilayered metal catalysts. Ion beam sputtering is used to deposit various metal layers sequentially. Underlayers of Al (2−20 nm) are shown to influence the growth characteristics with Fe or Ni used as active catalysts. The as-sputtered catalyst surface, characterized using atomic force and scanning tunneling microscopies, consists of nanometer scale (<10 nm) catalyst particles. High-resolution transmission electron microscopy and Raman analysis are used to characterize the MWCNTs. Optimization of the two layers allows growth of MWCNT towers on patterned and unpatterned substrates.

Introduction

Carbon nanotubes (CNT) have been the subject of intensive research recently because of their unique electronic properties and extraordinary mechanical properties. While there is no doubt that the single-walled nanotube is the highly desirable material, multiwalled carbon nanotubes (MWCNTs) are also investigated widely because of their potential as field emitters and electrodes. Inexpensive and scalable growth techniques are critical to realize these applications, and chemical vapor deposition (CVD) with the aid of transition-metal catalysts has emerged as a viable technique since it is amenable to grow nanotubes on patterned substrates and in vertically aligned arrays.[1,2] Numerous researchers have reported MWCNT growth by CVD using hydrocarbon (CH_4, C_2H_2, C_2H_4, etc.) or CO feedstock and Fe, Ni, or Co as catalysts supported on various substrates.[2−12] Continuous gas-phase CVD of MWCNTs aided by floating catalysts, generated in situ, has also been reported.[13,14]

The choices for the catalyst, substrate, and the method to transfer the catalyst to the substrate are critical to the success of CVD of nanotubes. In many cases, the catalyst precursor and structure-directing agents or other additives, if any, are in a solution which is evaporated and calcined to prepare the catalyst formulation on the substrate.[1,4−8] One problem with solution-based catalyst preparation techniques is the difficulty in confining the catalyst within patterns, particularly in small-feature sizes needed for device development. Another problem is the long time required for and the cumbersome nature of catalyst preparation. A typical solution-based procedure involves many of the following steps: mixing, dissolution, refluxing, separation, cooling, gel formation, reduction, and drying/annealing/calcination. Some of these steps take several hours to overnight processing. In contrast, physical deposition processes are quick, easy, and amenable to produce small patterns. For example, electron gun evaporation,[10] thermal evaporation,[11] pulsed laser deposition,[12] and magnetron sputtering[15] have been used in catalyst deposition. Nanochannel alumina templates made by anodization and followed by e-beam[2] or electrochemical[9] deposition have been helpful in growing highly ordered array of MWCNTs. Ion beam sputtering is used in the present work to deposit an underlayer of Al followed by an active catalyst layer of either iron or nickel.

The catalyst layer applied by physical processes in previous works[10−12,15] appears to be a thin film (under 100 nm) and smooth. However, apparently smooth films do not grow nanotubes, and catalyst nanoparticles are needed to enable nanotube growth.[16] Nanoparticle creation appears to be accomplished by pretreatment of the catalyst film with ammonia,[11,12] ion bombardment in a plasma environment,[15] or any other approach to break a film into small particles prior to starting the CVD process. In ammonia pretreatment, the treatment time, temperature, NH_3 flow rate, and substrate seem to influence the resulting particle size. In general, thinner catalyst films yield smaller particle sizes with little agglomeration.[12] There is evidence[10] that nucleation and growth of nanotubes increase with a decrease in catalyst layer thickness at a fixed growth temperature. In plasmas, particle creation is enabled by a pretreatment in an inert gas plasma prior to the introduction of the hydrocarbon into the growth chamber.[15] The treatment time, substrate bias (and hence the ion energy), and the starting film thickness control the size distribution of resulting particles. We have previously found that introduction of a metal underlayer (such as Al or Ir) under the active catalyst layer—instead of any form of pretreatment of the catalyst layer—appears to increase the surface roughness and to provide more active nucleation sites.[16] This approach is also the least time-consuming. Indeed in ref 16, we have successfully demonstrated growth of SWCNTs and shown that the density of the nanotubes can be varied by varying the thickness of the underlayer and the active catalyst layer. In this work, we extend this approach to grow MWCNT towers, and we discuss the results as a function of growth conditions and multilayer formulation.

Experimental Work

Ion beam sputtering is used for the deposition of an underlayer of Al followed by an active catalyst (Fe or Ni) to grow MWCNTs. The metals used in the experiments are 99.9+%

* To whom correspondence should be addressed. MS 239-4. Phone: 650-604-0236. Fax: 650-604-1088. E-mail: ldelzeit@mail.arc.nasa.gov.

† ELORET Corporation.

10.1021/jp0203898 CCC: $22.00 © 2002 American Chemical Society
Published on Web 05/14/2002

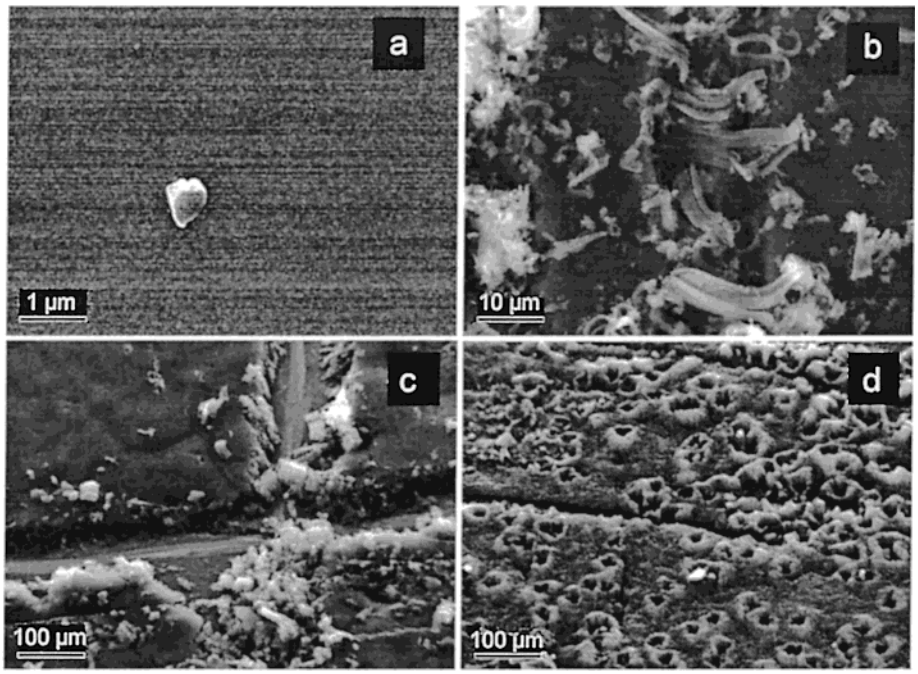

Figure 1. SEM images showing the effect of Fe layer thickness on MWCNT growth. (a) 1 nm, (b) 5 nm, (c) 10 nm, and (d) 20 nm. The Fe layer is deposited above a 20-nm Al underlayer on a silicon substrate.

pure and sputtered using a VCR Group Incorporated Ion Beam Sputterer (model IBS/TM200s). We have studied the growth of MWCNTs on a variety of substrates such as Si wafers, fused quartz, mica, highly oriented pyrolytic graphite (HOPG), and copper. The substrate with the catalyst formulation is inserted into the CVD reactor which consists of a quartz tube (1-in. diameter) within a high-temperature furnace and mass flow controllers.[8,16] Argon (Scott Specialty Gases, 99.999% pure, 1000 sccm) is used to purge the reactor while the furnace is heated to 750 °C. After the furnace reaches 750 °C, it is allowed an additional 10 min for the temperature to equilibrate. The gas flow is then switched to 1000 sccm of ethylene (Scott Specialty Gases, 99.999% pure) for 10 min. The gas flow is switched back to argon after the growth process to purge ethylene from the tube and to prevent back flow of air into the tube. The furnace is then allowed to cool below 300 °C before exposing the NTs to air. Exposure to air at elevated temperatures can cause damage to the NTs.

The nanotubes were characterized by scanning electron microscopy (SEM), transmission electron microscopy (TEM), and Raman spectroscopy. Raman spectra are taken with a System 2000 micro-Raman spectrometer (Renishaw) in the backscattering configuration. We use 2−3 mW laser power on the sample with a 1-μm focus spot, and a 50× objective is used for the microprobe. Most spectra are taken with 50% laser power at 10-s accumulation time. A 514-nm Argon ion laser is used for excitation. The spectral resolution is 4 cm^{-1} in the 100−2000 cm^{-1} window. Spectra are taken at least in three different spots to ensure the reproducibility for peak intensities. The spectrometer is calibrated with atomic emission from a neon lamp and checked by the silicon lines before the spectrum is taken.

Results and Discussion

We have previously shown that an underlayer of Al (10−20 nm) and a 1-nm thick Fe layer yield single-walled nanotubes with methane as the feedstock at a growth temperature of 900 °C.[16] Our initial attempts here utilized the same catalyst formulations and methane but at a lower growth temperature of 750 °C which resulted in a mixture of SWCNTs, MWCNTs, and filaments. This indicated the possibility to optimize the growth conditions for MWCNTs. When methane was replaced by ethylene at 750 °C, a greater success for growing MWCNTs was achieved with similar catalyst formulations. A theoretical analysis[17] of catalyzed nanotube growth indeed shows that lower temperatures (<900 °C) and higher supply of carbon (through the use of higher order hydrocarbons) favor production of MWCNTs over single-walled nanotubes. In the remainder of this work, growth conditions are fixed at 750 °C and 1000 sccm ethylene flow. Though in our previous work[16] we experimented with two underlayers (Al, Ir) and two catalysts (Fe, Mo) all together forming a multilayer structure, here we mostly restrict to a bilayer structure with Al as underlayer and either Fe or Ni as catalyst.

The effect of active layer thickness on nanotube growth is discussed first. Fixing the Al thickness at 20 nm on silicon wafers, the Fe layer is varied between 1 and 20 nm (Figure 1). Nanotubes do not grow when the Fe layer is only 1 nm. A sparse distribution of MWCNTs as clumps and islands appears when Fe thickness increases to 5 nm. With thicker Fe layers (10 and 20 nm), a continuous growth of MWCNTs as a vertically aligned tower is seen across the entire surface. We have also experimented with the addition of Mo to Fe as cocatalyst and found the performance to be equally good with and without Mo. From our previous work, an Al underlayer was absolutely necessary to initiate SWCNT growth on Fe catalysts[16] and a thickness of 10 nm maximized the nanotube growth. In the present work, when the Al underlayer is removed and only Fe is used, MWCNT growth is still observed. When the Fe is only 5 nm, only small clusters of nanotubes (not shown here) are seen which are not as dense but more evenly distributed across the entire surface compared to Figure 1b with the Al underlayer. The 10- and 20-nm Fe samples without the underlayer also exhibit good uniformity. However, as will be shown later, the underlayer allows easier optimization of the catalyst layer and prevents excess catalyst resulting in the growth of multiple, stacked layers of nanotubes.

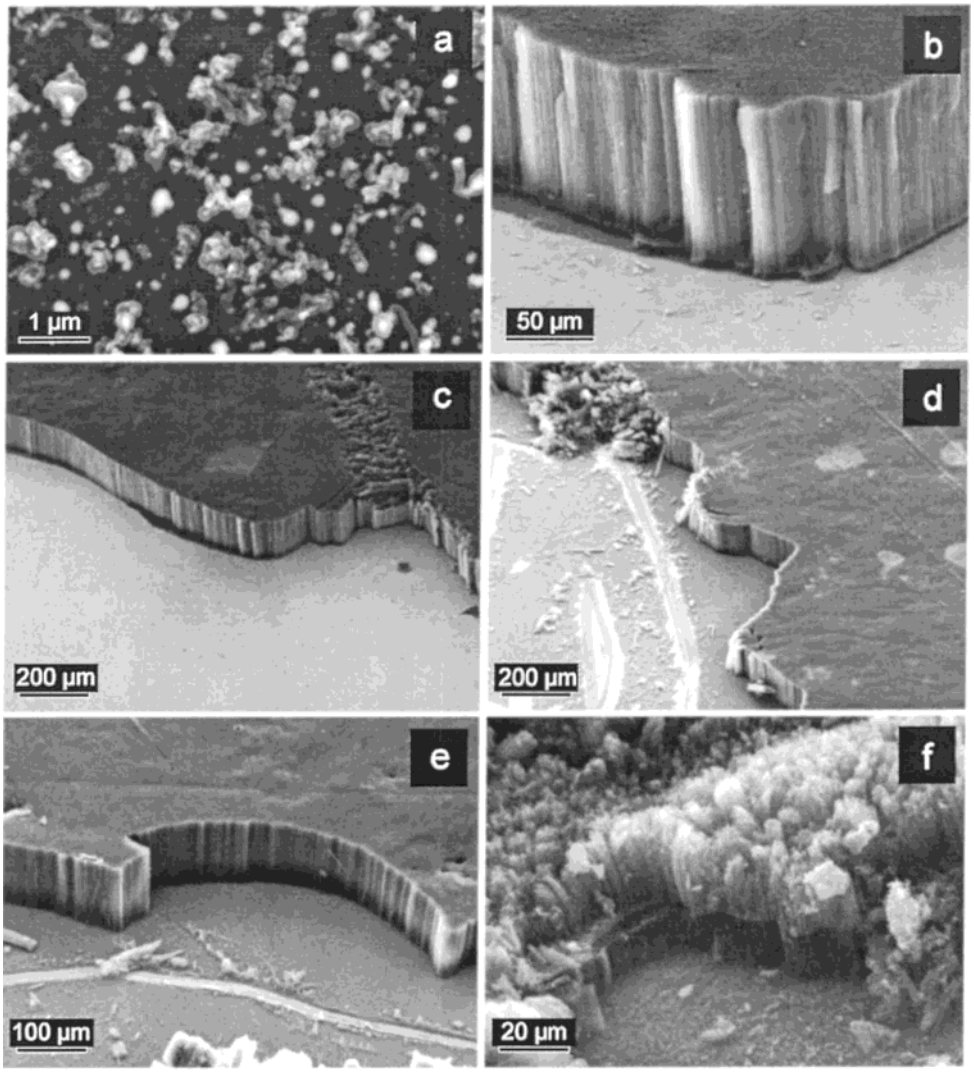

Figure 2. SEM images of MWCNT samples grown with nickel catalyst on a silicon substrate. (a) no nanotubes are seen for 10-nm Ni without an Al underlayer. In b−f, effect of Al underlayer thickness is shown, keeping Ni at 5 nm. (b) 20 nm, (c) 11 nm, (d) 6 nm, (e) 3.5 nm, and (f) 2 nm.

Nickel has been widely used as a catalyst in the growth of CNTs, and therefore we have investigated Ni also in the present work (see Figure 2). Nickel by itself, without the underlayer, does not seem to produce nanotubes regardless of thickness (5−20 nm). While this might at first be surprising, previous works using Ni guaranteed some form of creating particles via pretreatment, ion bombardment, and so forth. In our work, if an underlayer of Al (5−20 nm) is used with 5- or 10-nm nickel, then a MWCNT tower is produced as seen in Figure 2. If the thickness of the Al layer is decreased below 20 nm with Ni thickness kept at 5 nm, the MWCNT tower retains its integrity until the Al reaches 3.5 nm. The quality of the tower begins to degrade at an Al thickness of 2 nm and approaches the point when pure Ni without the underlayer fails to produce any nanotubes.

Our approach for the sequential deposition of various layers is amenable for integration with lithographic and shadow-masking techniques. We have used a 400-mesh TEM grid as a shadow mask and deposited the underlayer (20-nm Al) and catalyst layer (10-nm Fe) through this grid. This produces islands which are 50-μm square separated by 10 μm. Carrying out CVD on this pattern results in MWCNT towers which match the dimension of the mask, and the height of the towers is controlled by the growth duration as evidenced from the results in Figure 3. Examination of the edge region of the towers confirms that the boundary between the deposited and masked areas is well defined and preserved. The towers in Figure 3 are similar to the seminal CVD-produced MWCNT towers by Fan et al.[2] which used a porous silicon substrate produced by electrochemical etching followed by electron beam evaporation of Fe films and overnight annealing in air. The last step of overnight annealing in air was needed in ref 2 to create an iron oxide layer which plays an important role in preventing the porous openings from collapsing during CVD. In contrast, the deposition of the underlayer and catalyst layer in the present work was done in 5−20 min (depending on layer thickness and including the time needed to change the sputter target) with no other preparation or pretreatment. Though all the towers (Figures 2 and 3) themselves appear vertically aligned, high-magnification images (not shown here) reveal that the nanotubes making up the towers grow like "upwardly growing vines" and intertwine with their neighbors forming loose bundles as they grow. This is true regardless of the catalyst formulation. A typical TEM image of the MWCNT is shown in Figure 4.

We have conducted our investigations on a wide variety of substrates in addition to Si wafers, such as quartz, mica, HOPG, and copper. Quartz and mica yielded MWCNTs for all the catalytic formulations discussed above. Pure Fe on HOPG does not produce nanotubes since iron decomposes HOPG and the resulting oversupply of carbon coats the iron particles. When

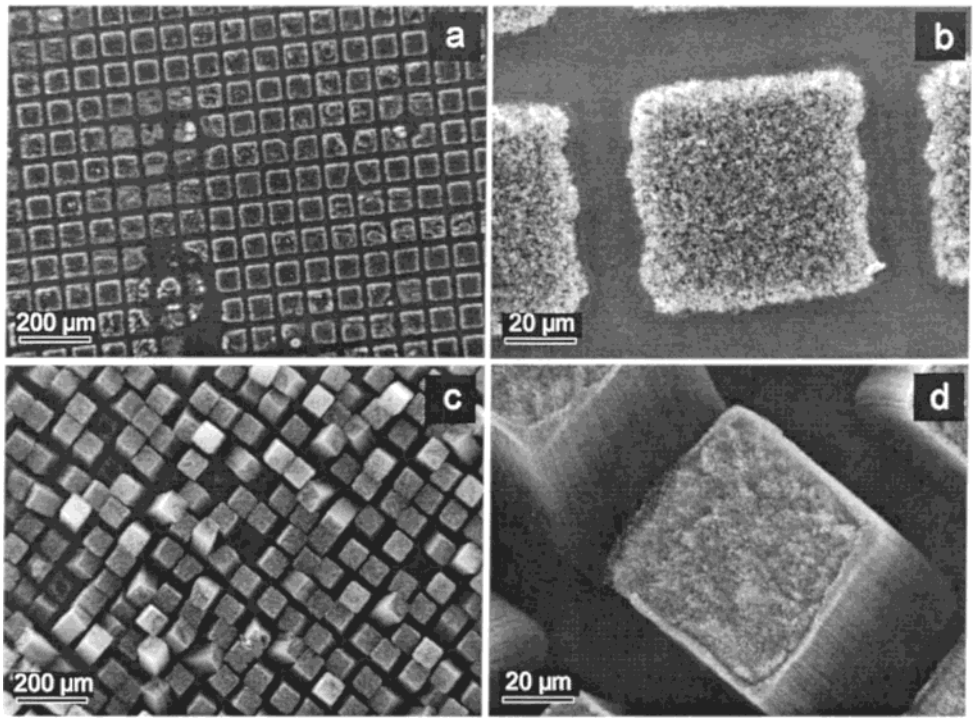

Figure 3. SEM images of MWCNTs deposited on a masked pattern. 20-nm Al and 10-nm Fe are deposited inside a 400-mesh TEM grid serving as the mask. Top images correspond to 1-min growth while the bottom images are after 10 min. The images on the right provide a close-up view of a single tower from the corresponding arrays on their left.

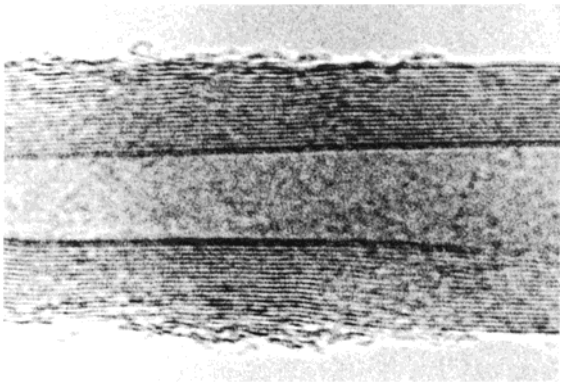

Figure 4. TEM image of a typical MWCNT from towers in Figure 3.

an Al underlayer is introduced under Fe, then the HOPG substrate is useful to grow nanotubes. Here the Al layer acts as a protective layer between Fe and HOPG. The copper substrate was the singular failure for growing nanotubes with or without an underlayer which may be due to the alloying of copper with other metals.

In acquiring the SEM images, a tweezer was used to scrape away a portion of the tower so that the height and morphology of the tower could be investigated as seen by the tweezer tracks in Figures 1, 2, and 5. In the process of doing this, it was noticed (see Figure 5) that not all of the nanotubes were being scraped away. In fact, nanotubes were removed only in the actual tracks of the tweezers. In the regions surrounding the tweezers tracks, the NTs were not all removed from the substrate but rather were just laid over. This signifies a very strong attachment of the CNTs to the surface, possibly even making ohmic contact. To remove all of the NTs, the surface would have to be scraped hard enough to shatter and remove the underlaying metal film. When a tower is scraped with a sharp object, the nanotubes come off the surface in "flakes". Examination of the flakes by TEM (not shown here) shows that the towers grow from a base-

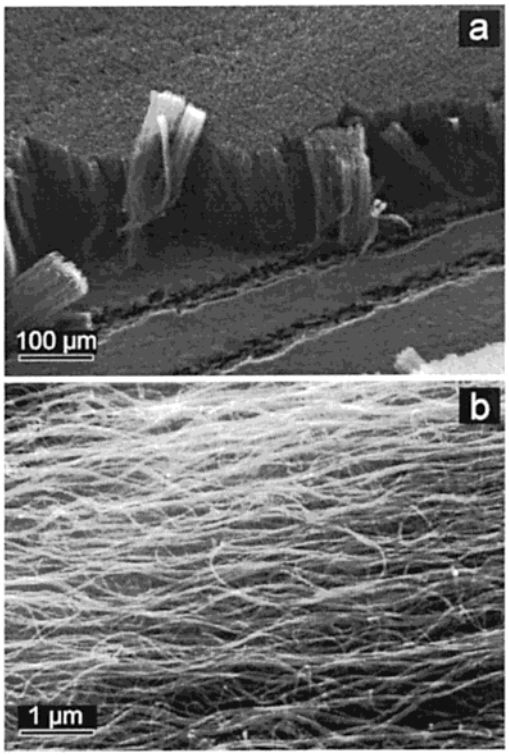

Figure 5. SEM images showing the attachment of nanotube towers to the surface. A tweezer was used to scrape the CNTs. (a) nanotubes removed on the tweezer tracks and (b) enlarged view of the area surrounding the tweezer tracks.

growth mechanism. This is evidenced by the MWCNTs growing from a thin-metal film at the base of the tower with no metal particle at the tip of the MWCNT. Further, since the MWCNTs are still fixed to the surface from which they have grown, there is no uncertainty as to which ends are the base and the top.

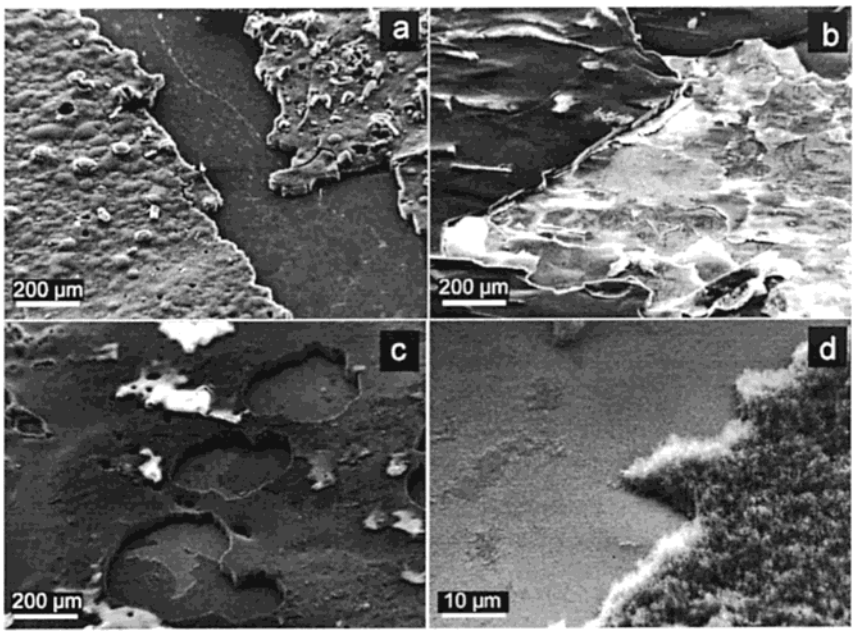

Figure 6. SEM images after the Scotch tape test of the MWCNT towers grown on (a) HOPG, (b) mica, and (c) Si. (d) Close-up view of the center hole in case (c) showing part of the catalyst film and nanotubes not removed by the tape because of its adhesion to the surface.

A "Scotch tape test" was used in an attempt to qualitatively determine the strength of the attachment of the CNTs to the surface. A piece of Scotch tape was firmly pressed to the surface of the tower and then pulled away (Figure 6). Of all the substrates investigated, the HOPG (Figure 6a) appears to have the weakest attachment of the tower. Large areas of the tower were removed from the HOPG surface, with about 50% of the tower remaining attached to the HOPG. The mica (Figure 6b) proved to be the next strongest which also had large areas of the tower removed, but unlike the HOPG sample, the underlaying mica also peeled off along with the nanotubes. Hence, it is not the CNT−mica connection that is the weak link, but rather the deteriorated mica. Mica begins to decompose around 500 °C. The Si wafer (Figure 6c) exhibits the strongest attachment of the tower to the substrate. After the tape test, only small areas of the tower were removed. Large areas of the adhesive were actually removed from the tape and remained attached to the top of the tower, which is an indication of the strength of attachment of CNTs to the silicon surface. In fact, the tower removed as much adhesive from the tape as the tape removed CNTs from the tower.

STM and AFM were used to characterize the as-sputtered metal deposits. We have previously used a SWCNT tip in an AFM and characterized an Ir surface showing 1−2-nm size particles.[18] A similar analysis of a 10-nm iron catalyst surface on Al underlayer using an AFM equipped with a SWCNT probe shows nanoparticles with diameter under 10 nm (Figure 7a). Figure 7c is an STM image of an as-sputtered nickel surface on Al underlayer again showing nanoscale particles. These results agree well with our previous characterization of a 1-nm Fe on 10-nm Al using TEM[16] which showed nanoscale particles as small as 2 nm. In addition, X-ray line scan across these particles revealed that they are indeed Fe particles. The nature of the surface under CVD conditions is not known. The melting point of bulk Al is about 660 °C though that of nanoparticles may be lower which may play a role in forming the catalyst nanoparticles. In the absence of in situ real-time imaging inside the CVD reactor, we examined an annealed surface just prior to deposition. Figure 7b shows AFM image of a (cooled) 10-nm Fe sample after it was heated in the CVD reactor for 15 min at 750 °C (just prior to introducing ethylene). This shows that the iron particles rearrange into larger islands which appear to be closely packed and measure the same size as the MWCNTs growing from this surface. Nolan et al.[19] indeed suggest, in their study on the thermodynamics and kinetics of carbon deposition, that alloying a catalyst with a noncatalytic metal increases the number of reactive sites through surface clusters.

If the catalyst layer tends to be too thick, the excess metal—unused as catalyst—ends up as contaminant at the top of the towers. Interestingly, this layer of metal serves to grow another layer of nanotubes above the original MWCNT tower, as shown in Figure 8. On occasion, even a third layer of nanotubes has been observed. It is possible to optimize the catalyst metal thickness to prevent such multilayer growth, and the use of the underlayer reduces the problem and makes the optimization easier. The underlayer helps to "glue" the catalyst to the substrate and to prevent any excess metal getting to the top of the towers. Figure 8b shows rectification of the situation in Figure 8a by adding a thin Cr layer (0.5 nm) as an underlayer.

As has been shown, both the Fe and Ni work well as catalysts to grow MWCNTs. However, small differences in growth characteristics between Fe and Ni do exist. After optimization of their respective growth conditions, the Ni provides a tower with a much more uniform growth and few defects within the tower. However, the removal of the excess contaminant metal, if any, from the top of the towers by optimization of the catalyst formula was by far more successful with the Fe formulations. Figure 9 shows Raman analysis of MWCNTs grown with Fe and Ni catalysts. Typical MWCNT Raman spectra show the active Raman tangential modes in the G-band[20] around 1600 cm^{-1} and the defect-induced mode around 1350 cm^{-1}. The two-phonon D-band secondary peak[21] appears at around 2690 cm^{-1}, and G-band appears at around 3220 cm^{-1}. In all the cases analyzed, the absence of peaks around 1700 cm^{-1} SWCNT signature suggests that the present process produces fairly pure MWCNTs. The silicon signals (520, 302, and 965 cm^{-1}) are from the Si substrate. In general, Ni produces fewer defects in the sidewall of the nanotubes. Figure 9 shows a larger relative intensity in the tangential modes around 1360 cm^{-1} in the nanotubes produced by the Fe catalyst than the Ni catalyst. This

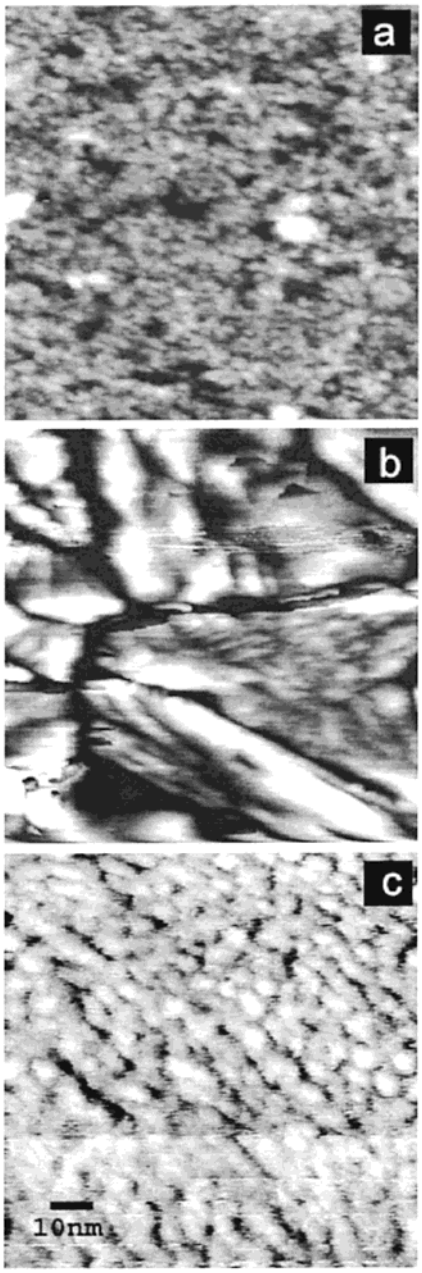

Figure 7. (a) AFM image of as-sputtered 10-nm iron catalyst on Al; the area shown is 150 nm × 150 nm. (b) AFM image of the catalyst surface in 7a after heating to 750 °C for 15 min and prior to the introduction of ethylene. The substrate was necessarily cooled before scanning with the nanoprobe. (c) STM image of as-sputtered nickel catalyst on Al.

mode presumably originates from several possible intrinsic graphitic defects: pentagons, heptagons, and so forth within the sidewalls and open ends of the nanotubes. The nanocrystalline carbon coming from the pyrolysis of CVD feedstock is another likely contributor to the D-band mode.

Concluding Remarks

We have demonstrated MWCNT growth from ethylene using CVD at 750 °C. Ion beam sputtering is used to sequentially deposit an underlayer (such as Al, Cr) and an active catalyst layer (such as Fe, Ni). Optimization of these two layers has been accomplished to grow MWCNT towers. The underlayer appears to perform one or more of the following functions. The underlayer may increase the surface roughness and provide more

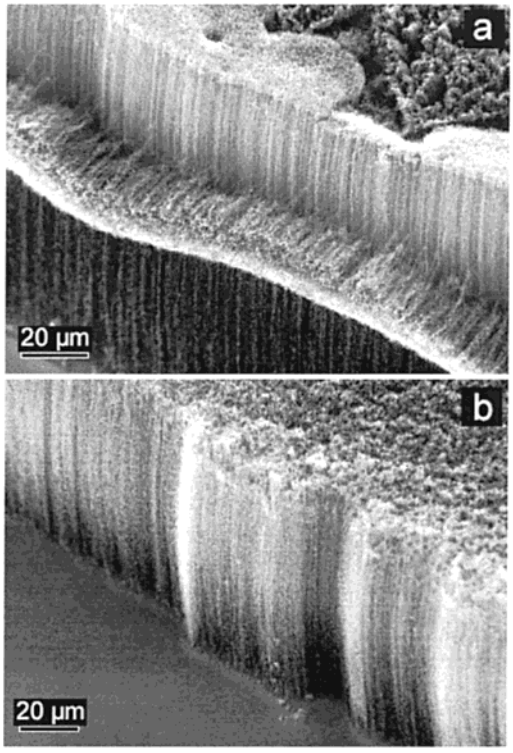

Figure 8. Effect of excessive catalyst metal and lack of underlayer on growth characteristics. (a) 10-nm Fe layer results in a double-layered MWCNT tower, (b) adding 0.5-nm Cr underlayer to 6-nm Fe results in a single tower.

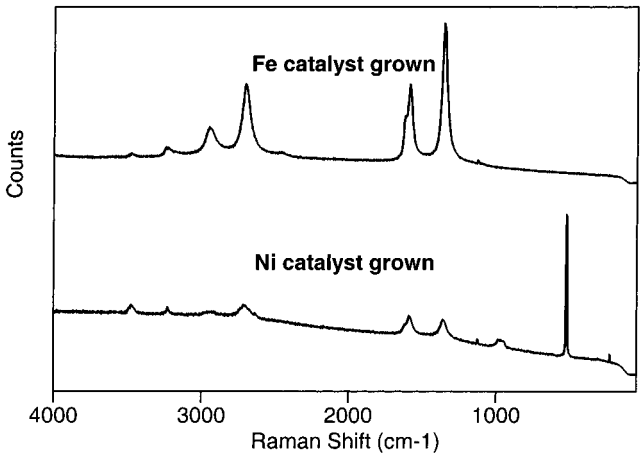

Figure 9. Raman spectra of MWCNT samples grown using Fe and Ni catalysts.

active nucleation sites; indeed, no growth is observed without Al when Ni is the active catalyst. Others who have used Ni successfully performed some form of pretreatment with ammonia or ion bombardment. The second role of a metallic underlayer such as Al may be the possibility to tune the final electrical conductivity of the structures in applications. In some cases, the metal underlayer helps to prevent the excess, unused catalyst metal layer from getting to the top of the towers and resulting in anomalous layered nanotube growth patterns. Finally, the metal underlayer can also play the role of a barrier between incompatible catalyst metal and substrate combination, which is the case with Fe on HOPG. Our approach to catalyst preparation is by far the simplest and quickest on the basis of a survey of the nanotube literature and to the best of our knowledge. The method is amenable for large areas as well as patterned wafers. We have demonstrated MWCNT growth on

a variety of substrates using this method. The MWCNT towers exhibit a very strong attachment to the silicon substrate.

Acknowledgment. This work was supported by NASA Ames Center for Nanotechnology and an NCI contract. Work by ELORET authors was funded by a NASA contract (NAS2-99092).

References and Notes

(1) Kong, J.; Soh, H. T.; Cassell, A. M.; Quate, C. F.; Dai, H. *Nature* **1998**, *395*, 878.
(2) Fan, S.; Chapline, M. G.; Franklin, N. R.; Tombler, T. W.; Cassell, A. M.; Dai, H. *Science* **1999**, *283*, 512.
(3) Jiao, J.; Nolan, P. E.; Seraphic S.; Cutler, A. H.; Lynch, D. C. *J. Electrochem. Soc.* **1996**, *143*, 932.
(4) Chen P.; Zhang, H. B.; Lin, G. D.; Hong, Q.; Tsai, K. R. *Carbon* **1997**, *35*, 1495.
(5) Pan, Z. W.; Xie, S. S.; Chang, B. H.; Wang, C. Y.; Lu, L.; Liu, W.; Zhou, W. Y.; Li, W. Z.; Qian, L. X.; *Nature* **1998**, *394*, 631.
(6) Kind, H.; Bonard, J. M.; Forro, L.; Kern, K.; Hernadi, K.; Nilsson, L.; Schlapbach, L. *Langmuir* **2000**, *16*, 6877.
(7) Cassell, A. M.; Meyyappan, M.; Han, J. *J. Nanopart. Res*. **2000**, *2*, 387.
(8) Cassell, A. M.; Verma, S.; Delzeit, L.; Meyyappan, M. *Langmuir* **2001**, *17*, 266.
(9) Li, J.; Papadopoulos, C.; Xu, J. M.; Moskovits, M. *Appl. Phys. Lett.* **1999**, *75*, 367.
(10) Wei, Y. Y.; Eres, G.; Merkulov, V. I.; Lowndes, D. H. *Appl. Phys. Lett.* **2001**, *78*, 1394.
(11) Lee, C. L.; Lyu, S. C.; Cho, Y. R.; Lee, J. H.; Cho, K. I. *Chem. Phys. Lett.* **2001**, *341*, 245.
(12) Sohn, J. I.; Choi, C. J.; Lee, S.; Seong, T. Y. *Appl. Phys. Lett.* **2001**, *78*, 3130.
(13) Sen, R.; Govindaraj, A.; Rao, C. N. R. *Chem. Phys. Lett.* **1997**, *267*, 276.
(14) Andrews, R.; Jacques, D.; Rao, A. M.; Derbyshire, F.; Qian, D.; Fan, X.; Dickey, E. C.; Chen, J. *Chem. Phys. Lett.* **1999**, *303*, 467.
(15) Choi, Y. C.; Shin, Y. M.; Lim, S. C.; Bae, D. J.; Lee, Y. H.; Lee, B. S.; Chung, D. C. *J. Appl. Phys.* **2000**, *88*, 4898.
(16) Delzeit, L.; Chen, B.; Cassell, A. M.; Stevens, R.; Nguyen, C.; Meyyappan, M. *Chem. Phys. Lett.* **2001**, *348*, 368.
(17) Karzow, H.; Ding, A. *Phys. Rev. B* **1999**, *60*, 11180.
(18) Nguyen, C. V.; Chao, K.-J.; Stevens, R.; Delzeit, L.; Cassell, A. M.; Han, J.; Meyyappan, M.. *Nanotechnology* **2001**, *12*, 363.
(19) Nolan, D.; Lynch, D. C.; Cutler, A. H. *J. Phys. Chem. B* **1998**, *102*, 4165.
(20) Thomsen, C. *Phys. Rev. B* **2000**, *61*, 4542.
(21) Moreno, J. M. C.; Yoshimara, M. *J. Am. Chem. Soc.* **2001**, *123*, 741.